Original Article

A magnetic resonance imaging-based lymph node regression grading scheme for nasopharyngeal carcinoma after radiotherapy

Hui Yang[1#^], Zhiying Liang[1#^], Jiahui Liang[1#], Di Cao[1^], Qin Cao[2], Feng Zhao[1], Weijing Zhang[1], Kit Ian Kou[3], Chunyan Cui[1], Lizhi Liu[1^], Haojiang Li[1^], Zexue Peng[4], Siyu Zhu[1^]

[1]State Key Laboratory of Oncology in South China, Guangdong Key Laboratory of Nasopharyngeal Carcinoma Diagnosis and Therapy, Guangdong Provincial Clinical Research Center for Cancer, Sun Yat-sen University Cancer Center, Guangzhou, China; [2]Department of Hepatobiliary Oncology, The People's Hospital of Yingcheng, Yingcheng, China; [3]Department of Mathematics, Faculty of Science and Technology, University of Macau, Macao, China; [4]Department of Radiology, Xiangya Changde Hospital, Changde, China

Contributions: (I) Conception and design: S Zhu, H Yang, Z Liang, D Cao; (II) Administrative support: Z Peng, Ha Li, L Liu, S Zhu; (III) Provision of study materials or patients: H Li, L Liu, D Cao, KI Kou; (IV) Collection and assembly of data: J Liang, Q Cao, F Zhao, W Zhang; (V) Data analysis and interpretation: H Yang, Z Liang, J Liang, D Cao; (VI) Manuscript writing: All authors; (VII) Final approval of manuscript: All authors.

[#]These authors contributed equally to this work.

Correspondence to: Siyu Zhu, PhD, MD. State Key Laboratory of Oncology in South China, Guangdong Key Laboratory of Nasopharyngeal Carcinoma Diagnosis and Therapy, Guangdong Provincial Clinical Research Center for Cancer, Sun Yat-sen University Cancer Center, 651 Dongfeng Road East, Guangzhou 510060, China. Email: zhusy@sysucc.org.cn; Zexue Peng, B.Med. Department of Radiology, Xiangya Changde Hospital, 1688 Moon Avenue, Wuling District, Changde 415000, China. Email: pzx755260@163.com.

Background: Among patients with nasopharyngeal carcinoma (NPC), there is no established method to distinguish between patients with residual disease that may eventually progress and those who have achieved cured. We thus aimed to assess the prognostic value of magnetic resonance imaging (MRI)-based lymph node regression grade (LRG) in the risk stratification of patients with NPC following radiotherapy (RT).

Methods: This study retrospectively enrolled 387 patients newly diagnosed with NPC between January 2010 and January 2013. A four-category MRI-LRG system based on the areal analysis of RT-induced fibrosis and residual tumor was established. Univariate analysis was performed using the Kaplan-Meier method, and comparisons were conducted via the log-rank test. Multivariate analyses were conducted using Cox regression models to calculate the hazard ratios (HRs) with 95% confidence intervals (CIs) and adjusted P values. Survival curves were calculated using the Kaplan-Meier method and compared using the log-rank test.

Results: The sum of MRI-LRG scores (LRG-sum) was an independent prognostic factor for progression-free survival (PFS) (HR 2.50, 95% CI: 1.28–4.90; P<0.001). LRG-sum ≤9 and >9 showed a poorer 5-year PFS rate than did LRG-sum ≤2 (66.1%, 42.9%, and 77.6%, respectively; P<0.001). A survival clustering analysis-based decision tree model showed more complex interactions among LRG-sum and pretreatment and post-RT Epstein-Barr virus (EBV) DNA, yielding four patient clusters with differentiated disease progression risks (5-year PFS rates of 89.5%, 76.4%, 57.6%, and 27.8%, respectively), which showed better risk stratification than did post-RT EBV DNA alone (P<0.001).

Conclusions: The MRI-LRG system adds prognostic information and is a potentially reliable, noninvasive means to stratify treatment modalities for patients with NPC.

^ ORCID: Hui Yang, 0009-0003-2033-0568; Zhiying Liang, 0000-0002-8311-5393; Di Cao, 0009-0000-0794-6139; Lizhi Liu, 0000-0002-3977-0518; Haojiang Li, 0000-0001-5854-3989; Siyu Zhu, 0000-0002-0839-2972.

Keywords: Nasopharyngeal carcinoma (NPC); risk stratification; lymph node regression grade (LRG); Epstein-Barr virus DNA (EBV DNA); postradiotherapy

Submitted Feb 21, 2024. Accepted for publication Jun 18, 2024. Published online Jul 17, 2024.
doi: 10.21037/qims-24-275
View this article at: https://dx.doi.org/10.21037/qims-24-275

Introduction

Radiotherapy (RT) is the primary treatment for patients with early-stage nasopharyngeal carcinoma (NPC), and combined chemotherapy is generally considered for patients with advanced-stage disease (1). Local recurrence and distant metastasis remain the major disease failures in patients with advanced NPC (2,3). Following treatment with curative RT or combined chemoradiotherapy (CRT), there is no established method to distinguish between patients with residual disease that may eventually progress and those who are cured.

The clinical guidelines for adjuvant chemotherapy are mainly based on the pretreatment tumor-node-metastasis (TNM) staging system. Patients with stages III and IV NPC are generally at high risk and are recommended to undergo adjuvant chemotherapy; however, the survival benefit does not increase with adjuvant chemotherapy (4-7). Excessive adjuvant chemotherapy often results in substantial toxicities, with trials investigating the addition of adjuvant therapy to CRT reporting mixed results (8,9). In NPC, detectable plasma Epstein-Barr virus (EBV) DNA after RT reflects minimal residual tumor load, which is significantly correlated with poor survival (10-12). However, a randomized controlled trial on adjuvant chemotherapy (NPC-0502) demonstrated that patients with detectable EBV DNA after RT did not benefit from adjuvant chemotherapy (13). Hence, selecting adjuvant treatment candidates merely based on detectable post-RT plasma EBV DNA is inadequate for precisely identifying those at the highest risk.

Tumor response, based mainly on the Response Evaluation Criteria in Solid Tumors (RECIST) 1.1 criteria, is an independent predictor of survival outcomes in patients with NPC following RT (14). Nevertheless, precisely assessing treatment response and predicting patient prognosis according to a unidimensional criterion for NPC with irregular lesions is difficult. A tumor regression grading (TRG) system based on the qualitative assessment of histologic changes in the resected specimen is an important prognostic predictor of clinical outcomes in rectal cancer (15). A similar magnetic resonance imaging (MRI)-based TRG system that uses the principles of histologic response and low-signal intensity appearance of fibrosis on T2-weighed images (T2WI) has also been proposed (16,17), with a reliable prognostic factor for predicting survival outcomes in rectal cancer (17,18). Patel *et al.* demonstrated that for rectal cancer, the relationship of the MRI-TRG system with histopathology was stronger than of RECIST (19). The influence of the therapeutic response of primary tumors on prognosis has been widely studied in NPC; nonetheless, metastatic lymph nodes (LNs) have received limited attention. Slow regression or residual nodal disease after definitive RT in these patients is associated with poor survival outcomes (20,21). MRI is recommended for LN response assessment following RT in patients with NPC.

This study proposes a four-category MRI LN regression grading (LRG) system based on the areal analysis of RT-induced fibrosis and the residual tumor to assess the treatment response of metastatic LNs to RT and investigate its prognostic value for NPC after RT. Furthermore, we developed a practical clinical tool by integrating the MRI-LRG system and plasma EBV DNA levels to accurately identify patients with NPC with varying risk profiles for individualized therapeutic strategies. We present this article in accordance with the STROBE reporting checklist (available at https://qims.amegroups.com/article/view/10.21037/qims-24-275/rc).

Methods

Patients and follow-up

This study included 387 patients with newly diagnosed NPC admitted to the Sun Yat-sen University Cancer Center between January 2010 and January 2013. This study was conducted in accordance with the Declaration of Helsinki (as revised in 2013) and was approved by the Medical Ethics Committee of Sun Yat-Sen University Cancer Center (approval number: B2019-222-01). The requirement for informed consent was waived due to the retrospective nature of the study.

The inclusion criteria were the following: (I) NPC confirmed by a pathological examination, (II) treatment with intensity-modulated radiotherapy (IMRT), (III) contrast-enhanced MRI performed before any treatment and 3–4 months after RT, (IV) patients with complete clinical information, and (V) patients without distant metastasis. Patients with N0 stage disease, primary distant metastasis, and concurrent tumors in other parts of the body and those lost to follow-up were excluded.

All included patients underwent assessments every 3 months during the first 2 years of follow-up and biannually thereafter. The primary endpoint was progression-free survival (PFS). Other survival outcomes, including overall survival (OS), distant metastasis-free survival (DMFS), and local recurrence-free survival (LRFS), were calculated from the date of therapy initiation to the date of the occurrence of a relevant event or the last follow-up visit.

All participants underwent a complete assessment consisting of hematological and biochemical tests, a physical examination, fiberoptic nasopharyngoscopy, chest radiography, nasopharyngeal and neck MRI, abdominal ultrasonography, and positron emission tomography-computed tomography before treatment.

Imaging acquisition

Patients underwent MRI scanning with a 1.5-T superconducting system (Signa CV/I, GE HealthCare, Chicago, IL, USA) or a 3.0-T superconducting system (MAGNETOM Trio Tim, Siemens Healthineers, Erlangen, Germany) from the suprasellar cistern to the inferior margin of the sternoclavicular joint. Gadopentetate dimeglumine (Magnevist, Bayer Schering Pharma AG, Berlin, Germany) was used for contrast-enhanced imaging at a dose of 0.3 mL/kg and a flow rate of 1 mL/s. Independent three-plane acquisition (axial, coronal, and sagittal planes) was performed for T1-weighted images (T1WI) and contrast-enhanced images. Only the axial plane was acquired for T2WI. Fat saturation was applied for the coronal contrast-enhanced images. The respective scanning parameters for T1WI and T2WI were a repetition time of 540 and 4,000 ms, respectively, and an echo time of 11.8 and 99 ms, respectively. The axial fast spin echo (FSE) T2WI sequences had a field of view (FOV) of 240 mm × 240 mm and a matrix size of 384×320. The section thicknesses were 2 mm for the sagittal or coronal planes and 5 mm for the axial planes, with a 1-mm interval. The Appendix 1 includes a detailed summary of the MRI acquisition parameters, as outlined in a previous study (22).

Treatments for NPC

All patients underwent IMRT. Induction chemotherapy or concurrent CRT (CCRT) was administered according to the eighth edition of the American Joint Committee on Cancer (AJCC) staging system; the institutional protocol has been described elsewhere (23).

Patients with stages II–IV NPC received CCRT, and induction chemotherapy was optional according to the clinicians' protocols: 13 (3.4%) patients received RT alone, 126 (32.6%) received CCRT alone, and 248 (64.0%) received induction chemotherapy + CCRT. The Appendix 1 provides detailed information regarding IMRT, CCRT, and induction chemotherapy according to a previous study (24).

MRI assessment

All patients underwent MRI before treatment and 3–4 months after RT. Information regarding the MRI procedure is provided in the Appendix 1. All MR images were independently reviewed by three experienced radiologists (L.L., H.L., and C.C., with 18, 10, and 9 years of experience in head-and-neck cancer, respectively) who were blinded to the patients' clinical characteristics and outcomes. We evaluated the signal intensity of residual LNs on T2WI as follows: high, similar signal intensity to the signal intensity of the cerebrospinal fluid; low, similar or lower signal intensity than the signal intensity of the muscle; and intermediate, a signal intensity between that of the cerebrospinal fluid and the muscle. LRG was evaluated 3–4 months after RT on T2WI under the following conditions: RT-induced LN fibrosis and the residual tumor were outlined on the axial T2WI using Photoshop version 21.0.0 software (Adobe, San Jose, CA, USA), and LRG was performed at the layer with the widest diameter of each residual LN in the axial plane. Zones with intermediate or high T2WI signals were considered residual tumors. In contrast, areas with low T2WI signals were considered fibrosis (25). The proportion of residual tumors was assessed using the following formula: tumor area/(tumor area + fibrosis area) × 100%. The percentage of MRI-detected residual tumor area was assumed to correlate with the patient's response to RT and survival outcomes.

Based on our hypothesis, a four-category MRI-LRG system was proposed for the noninvasive assessment of LN response to RT according to previous studies (26,27). The

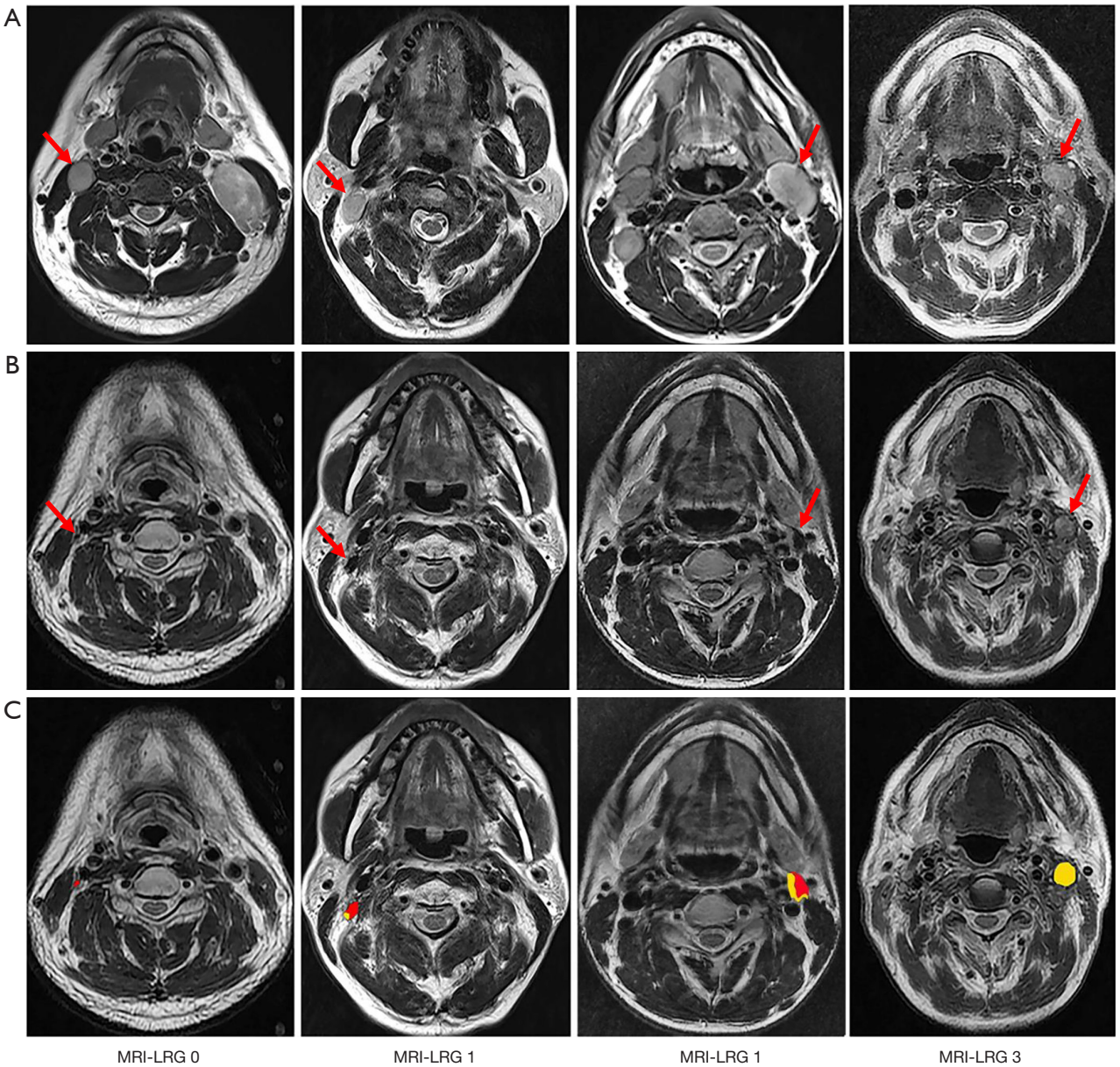

Figure 1 Representative images of the MRI-LRG categories. The axial plane of T2-weighted images for MRI-LRG 0 to MRI-LRG 3 category patients are displayed in the four columns from left to right, respectively. (A) The metastatic lymph node at the representative axial plane of a T2-weighted image before treatment (red arrows). (B) The metastatic lymph node at the representative axial plane of a T2-weighted image 3–4 months following the completion of radiotherapy (red arrows). (C) The T2 image [shown in (B)] with areas of fibrosis (red section) and residual tumor (yellow section) highlighted using Photoshop software. MRI, magnetic resonance imaging; LRG, lymph node regression grade.

MRI-LRG categories were defined as follows: MRI-LRG 0, good response (absence of residual tumor or the tumor disappearing entirely); MRI-LRG 1, moderate response (residual tumor accounting for ≤25%); MRI-LRG 2, minimal response (residual tumor accounting for 25–50%; and MRI-LRG 3, poor response (residual tumor accounting for >50%) (*Figure 1*). All radiologically suspected LNs before treatment were assessed, and each LN was scored from 0 to 3 for regression degree according to the MRI-LRG system. Owing to the variability of LN responses

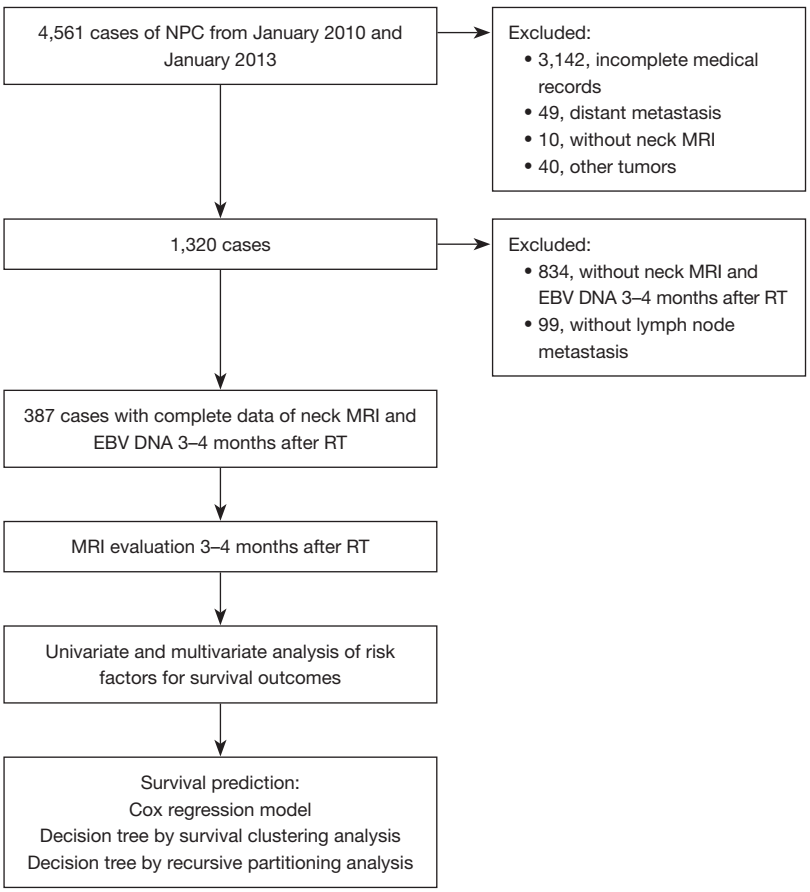

Figure 2 Flowchart of the study design and patient selection process. NPC, nasopharyngeal carcinoma; MRI, magnetic resonance imaging; EBV, Epstein-Barr virus; RT, radiotherapy.

observed in patients, the sum score of the MRI-LRG of each counted LN was calculated as the final LRG score (LRG-sum) to assess the LN response for each patient.

Statistical analysis

Differences in the clinical features were analyzed using the chi-squared test or Fisher exact test. The kappa statistic was used to assess the interreader reliability in the evaluation of LRG. The exhaustion method identified the best cutoff values for LRG-sum, pretreatment EBV DNA, and post-RT EBV DNA. Univariate analysis was performed with the Kaplan-Meier method, and comparisons were completed via the log-rank test. Multivariate analyses were conducted using Cox regression models to calculate the hazard ratios (HRs) with 95% confidence intervals (CIs) and adjusted P values. The concordance indices (C-indices) were calculated to compare the predictive performance of the prognostic models. The *U*-statistics test was used to compare two C-indices and evaluate the P values via the rcorrp.cens function in the "Hmisc" package of R (The R Foundation for Statistical Computing), with bootstraps of 1,000 resamples being used. Survival curves were plotted using the Kaplan-Meier method and were compared using the log-rank test. Statistical tests were conducted using packages from R version 4.0.1. Statistical significance was defined as a two-sided P value <0.05.

Results

Clinical characteristics, survival outcomes, and univariate analysis

We included 387 eligible patients with NPC. *Figure 2* presents the study flowchart. After a median follow-up of 64.1 months, 44 (11.4%) patients developed local recurrence, 58 (15.0%) developed distant metastasis, 99 (25.6%)

Table 1 Clinical characteristics of the patients and univariate analysis

Variables	Value (N=387)	5-year PFS, %	P value
Age (years)	46 (13–75)	–	0.794
Sex			0.018
Male	281 (72.6%)	76.23	
Female	106 (27.4%)	64.23	
Histologic type			0.175
WHO type 1/2	14 (3.6%)	56.25	
WHO type 3	373 (96.4%)	73.64	
T stage			0.425
T1	66 (17.1%)	78.28	
T2	52 (13.4%)	77.11	
T3	162 (41.9%)	72.55	
T4	107 (27.6%)	67.86	
T stage[2]			0.130
T1–2	118 (30.5%)	77.93	
T3–4	269 (69.5%)	70.68	
N stage			0.074
N1	263 (68.0%)	75.70	
N2	89 (23.0%)	69.79	
N3	35 (9.0%)	60.88	
N stage[2]			0.036
N1	263 (68.0%)	75.70	
N2–3	124 (32.0%)	67.25	
AJCC stage			0.455
II	87 (22.5%)	75.97	
III	169 (43.7%)	74.49	
IV	131 (33.9%)	68.95	
Treatment			0.673
RT	13 (3.4%)	81.82	
CCRT	126 (32.6%)	71.84	
IC + CCRT	248 (64.1%)	73.05	
Pretreatment EBV DNA (10^3 copies/mL)			0.003
<1	68 (17.6%)	87.43	
<26	209 (54.0%)	73.48	
≥26	110 (28.4%)	62.85	
Post-RT EBV DNA (10^3 copies/mL)			<0.001
0	330 (85.3%)	77.98	
≤2	28 (7.2%)	57.37	
>2	29 (7.5%)	27.79	
LRG-sum			<0.001
≤2	278 (71.8%)	77.59	
≤9	86 (22.2%)	66.09	
>9	23 (5.9%)	42.86	

The 5-year PFS was calculated with the Kaplan-Meier method, and the P values were calculated using the log-rank test. As the classical T and N stages were not significantly related to PFS in the univariate analysis, the T1 and T2 stages were combined into the T1–2 category, while T3 and T4 stages were combined into the T3–4 category to generate a new T stage[2]. The N2 and N3 stages were combined into the N2–3 category to generate a new N stage[2]. PFS, progression-free survival; WHO, World Health Organization; AJCC, American Joint Committee on Cancer; RT, radiotherapy; CCRT, concurrent chemoradiotherapy; IC, induction chemotherapy; EBV, Epstein-Barr virus; LRG, lymph node regression grade.

developed progression, and 51 (13.2%) patients died.

In terms of the confounding factors: sex (P=0.018), N stage (P=0.036), and pretreatment (P=0.003) and post-RT EBV DNA levels (P<0.001) were correlated with PFS; meanwhile, age (P=0.026), T stage (P=0.091), and pretreatment (P=0.006) and post-RT EBV DNA levels (P<0.001) were correlated to OS; finally, N stage (P=0.017) and pretreatment (P=0.012) and post-RT EBV DNA levels (P<0.001) were correlated with DMFS (univariate analysis: *Table 1*; multivariate analysis: *Table 2* and Table S1).

Independence and reliability of the MRI-based LRG

In the assessment of the reliability of MRI-based LRG, the kappa coefficients for interreviewer identification were 0.92, 0.87, 0.82, and 0.83 for the diagnosis of LRG 0, LRG 1, LRG 2, and LRG 3, respectively. Univariate and multivariate analyses demonstrated that the LRG-sum was independently associated with PFS (P<0.001), DMFS (P=0.001), and LRFS (P=0.010) (*Tables 1*,*2*, and Table S1, respectively). Furthermore, nomogram model A incorporating LRG had a higher C-index for PFS prediction than that of the model without LRG (Figure S1,

Table 2 Stepwise multivariate analysis of the independent risk factors for PFS

Variables	HR (95% CI)	P value
LRG-sum		
≤2	Reference	
≤9	1.41 (0.89–2.24)	0.138
>9	2.50 (1.28–4.90)	0.007
Pretreatment EBV DNA (10^3 copies/mL)		
<1	Reference	
<26	1.96 (0.96–4.01)	0.064
≥26	2.62 (1.23–5.59)	0.013
Post-RT EBV DNA (10^3 copies/mL)		
0	Reference	
≤2	2.21 (1.17–4.20)	0.015
>2	5.52 (3.27–9.31)	<0.001
Sex		
Male	Reference	
Female	1.54 (1.02–2.34)	0.040
N stage[2]		
N1	Reference	
N2–3	1.06 (0.67–1.65)	0.812

Hazard ratios and adjusted P values were calculated using the multivariate Cox regression models. LRG-sum, pretreatment EBV DNA, post-RT EBV DNA, sex, and N stage[2], all confounding variables with P<0.05 according to univariable analysis in *Table 1*, were tested for PFS. These factors were included in the final Cox regression model and used for the development of the nomogram. LRG-sum, pretreatment EBV DNA, and post-RT EBV DNA were confirmed as significantly independent factors associated with 5-year PFS (P=0.007, P =0.013, and P<0.001, respectively) and were the main research variables in this study. PFS, progression-free survival; HR, hazard ratio; CI, confidence interval; LRG, lymph node regression grade; EBV, Epstein-Barr virus; RT, radiotherapy.

Table S2). These results imply that LRG may be used as a potential biomarker for predicting survival outcomes.

Clinical utility of MRI-based LRG

To further exploit the clinical value of MRI-based LRG in risk stratification in NPC, Kaplan-Meier analysis was performed to evaluate the survival differences based on LRG-sum, post-RT EBV DNA, and pretreatment EBV DNA (*Figure 3*). The 5-year PFS rates of LRG-sum ≤9 and LRG-sum >9 were poorer than that of LRG-sum ≤2 (66.1%, 42.9%, and 77.6%, respectively, P<0.001). Among 387 patients, post-RT EBV DNA was undetectable in 330 (85.3%) (Table S3). Among these patients, 16 (5.8%) had an LRG-sum score >9, which was associated with an unfavorable prognosis as compared with patients with an LRG-sum score ≤9. These results indicate that LRG may help facilitate risk stratification based solely on detectable post-RT EBV DNA.

Using a supervised statistical clustering of disease relapse risks (12), we further binned the nine subgroups (classified by LRG-sum, post-RT EBV DNA, and pretreatment EBV DNA) into different prognostic phenotypes based on the intergroup PFS HR (HR_{PFS}) and classified the patients into four clusters (Figure S2). These clusters showed significantly different intergroup prognoses between all clusters, except between clusters 1 and 2. The 5-year PFS rates for clusters 1–4 were 89.5%, 76.4%, 57.6%, and 27.8%, respectively (*Figure 4A*, Figure S3). Based on the abovementioned survival clustering, we proposed a decision tree model for the risk stratification of patients with NPC (*Figure 4B*).

The PFS of the moderate risk group in the survival clustering analysis-based decision tree was comparable with that of post-RT EBV DNA model (5-year PFS rate 57.6% *vs.* 57.4%), and more patients who could potentially receive a more aggressive treatment strategy in time were identified (11.4% *vs.* 7.2%).

Furthermore, the PFS rate of the survival clustering analysis-based decision tree low-risk group was higher than that of the post-RT EBV DNA model (5-year PFS 89.5% *vs.* 78.0%). Moreover, 15.8% (61/387) of patients who could potentially receive a more refined and cost-effective surveillance strategy were identified, which was a higher proportion than that of the medium-low risk group in the survival clustering analysis model and low-risk group in the post-RT EBV DNA model. *Table 3* presents the detailed predicted 5-year PFS rates.

Discussion

To the best of our knowledge, this study is the first to apply an MRI-based LRG system for the treatment response assessment and risk stratification of patients with NPC following RT. This four-category MRI-LRG system, based on the principle of fully reflecting LN response to RT, quantitatively evaluated LNs by calculating the proportion

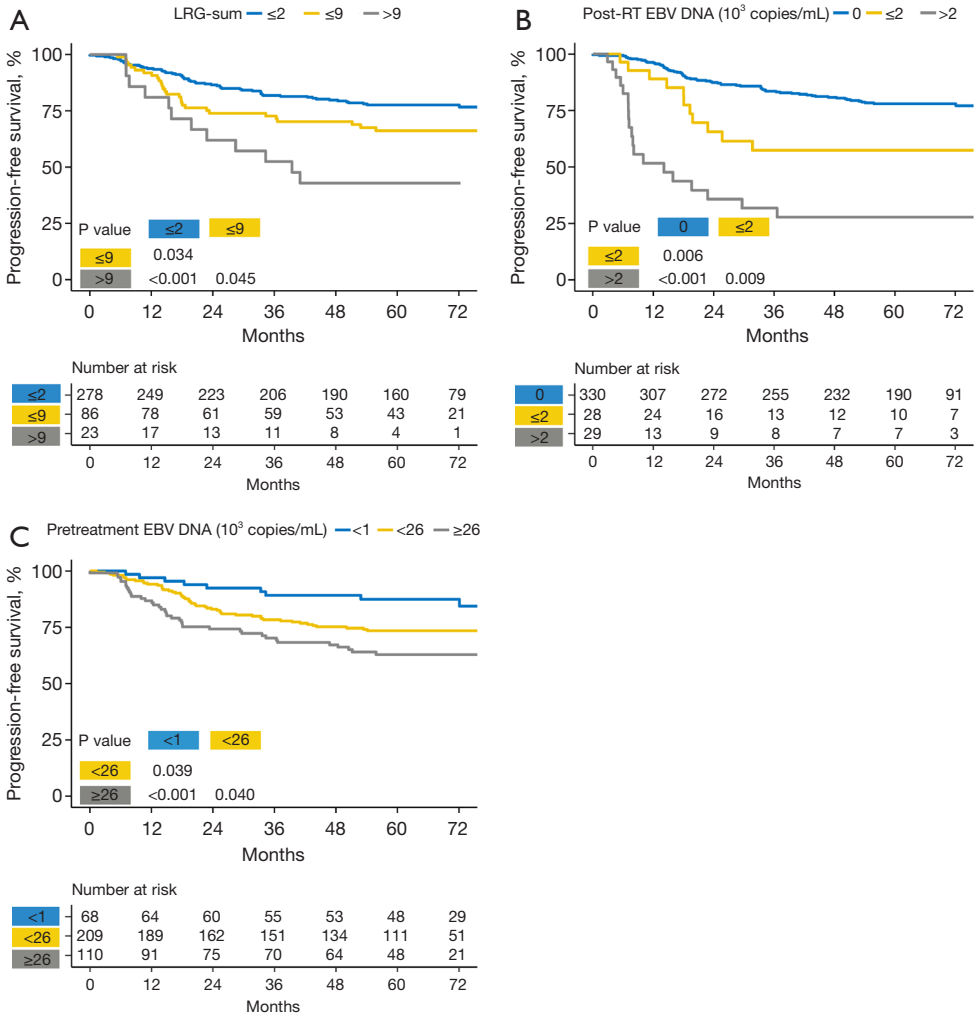

Figure 3 Survival outcomes for PFS. Kaplan-Meier survival plot of PFS based on (A) LRG-sum, (B) post-RT EBV DNA (B), and (C) pretreatment EBV DNA. LRG, lymph node regression grade; RT, radiotherapy; EBV, Epstein-Barr virus; PFS, progression-free survival.

of residual tumor lesions and RT-induced fibrosis. LRG-sum was found to be an independent prognostic factor for PFS, DMFS, and LRFS in patients with NPC. Moreover, the survival clustering analysis-based decision tree model finely integrating LRG-sum, pretreatment EBV DNA, and post-RT EBV DNA showed better risk stratification than did post-RT EBV DNA alone in NPC. Thus, this model offers more accurate prognosis prediction and personalized treatment selection for patients with NPC after RT.

In this study, we developed an LRG-score system and demonstrated that the LRG-sum based on MRI evaluation was an independent prognostic marker for survival outcomes in patients with NPC, which is consistent with the results of a previous study on rectal cancer (28). The therapeutic regimens for NPC are RT or CCRT without surgery as acquiring histopathological results of all metastatic LNs as in rectal cancer is impossible since retropharyngeal LNs are located relatively deep anatomically (29), and cervical LN biopsy raises potential safety concerns among patients (30). Hence, we used an LRG-score system based on MRI, which helped to improve the predictive accuracy for survival outcomes in NPC. Furthermore, our findings revealed that pretreatment and post-RT plasma EBV DNA levels were independent prognostic factors for patients with NPC, which is consistent with previous findings (12,13,31). Pretreatment EBV DNA improves the predictive efficacy of the TNM staging system (32), and post-RT EBV DNA contains predictive information that can better predict early disease

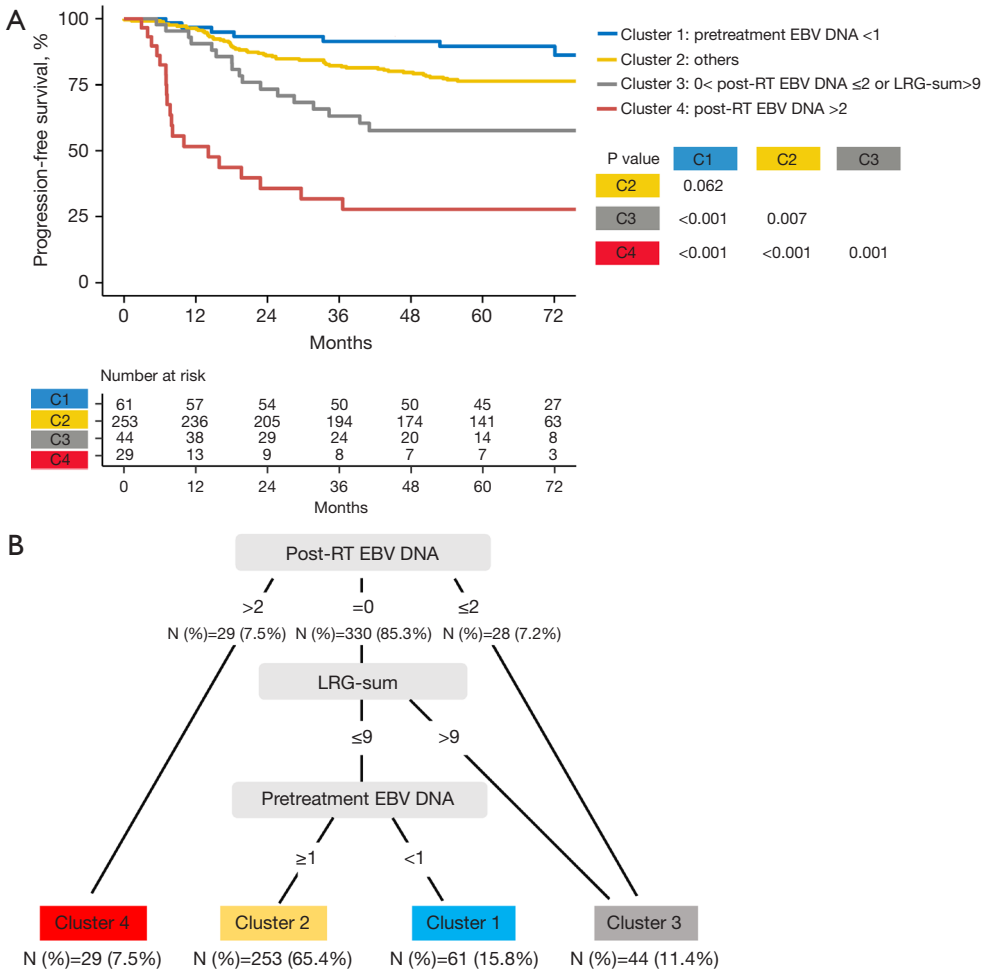

Figure 4 Survival clustering analysis-based decision tree. (A) Kaplan-Meier plot of PFS for the four clusters classified according to the intergroup HRPFS based on LRG-sum, post-RT EBV DNA, and pretreatment EBV DNA. (B) Decision tree model based on the abovementioned survival clustering analysis. EBV, Epstein-Barr virus; RT, radiotherapy; LRG, lymph node regression grade; PFS, progression-free survival; HR, hazard ratio.

events following RT in NPC than can the conventional TNM staging system (33). However, post-RT EBV DNA alone is inadequate in selecting high-risk patients for adjuvant treatment (13). Accordingly, we developed a decision tree model using a supervised statistical clustering of disease relapse risks classified by LRG-sum, post-RT EBV DNA, and pretreatment EBV DNA.

The survival clustering analysis-based decision tree model advantageously used LRG-sum, pretreatment EBV DNA, and post-RT EBV DNA to stratify patients according to their degree of inter-similarities in prognosis into nine subgroups (*Figure 4*, Figure S2) and showed better survival segregation than did the post-RT EBV DNA model. Both completed and ongoing adjuvant trials have elected to stratify patients via post-RT EBV DNA (NCT00370890, NCT02135042, NCT02958111, NCT03427827, NCT03403829, NCT02363400, and NCT02874651, ClinicalTrials.gov). However, most of these studies have stratified patients according to detectable and undetectable post-RT EBV DNA, ignoring the imbalances in post-RT EBV DNA levels among the therapeutic groups that might influence outcomes. Our study stratified patients with NPC into post-RT EBV DNA = 0, ≤2, and >2×10^3 copies/mL, which identified the highest-risk patients (>2×10^3 copies/mL) expected to benefit from a more aggressive form of therapy. Patients with post-RT EBV DNA ≤2×10^3 copies/mL were assigned to the moderate risk group.

Furthermore, patients with post-RT EBV DNA

Table 3 Prognostic models for the prediction of 5-year PFS

Prognostic models	Patient No. (%)	5-year PFS	HR (95% CI)	P value[#]
Post-RT EBV DNA (10^3 copies/mL)				
0 (low risk)	330 (85.3)	78.0%	Reference	
≤2 (moderate risk)	28 (7.2)	57.4%	2.21 (1.17–4.20)	0.015
>2 (high risk)	29 (7.5)	27.8%	5.52 (3.27–9.31)	<0.001
Survival clustering analysis-based decision tree				
Cluster 1 (low risk)	61 (15.8)	89.5%	Reference	
Cluster 2 (medium-low risk)	253 (65.4)	76.4%	2.06 (0.94–4.52)	0.072
Cluster 3 (moderate risk)	44 (11.4)	57.6%	4.22 (1.75–10.19)	0.001
Cluster 4 (high risk)	29 (7.5)	27.8%	12.61 (5.28–30.09)	<0.001

Survival clustering analysis-based decision tree included three risk factors: LRG-sum, pretreatment EBV DNA, and post-RT EBV DNA. [#], the Kaplan-Meier method was used to calculate the 5-year PFS, while multivariate Cox regression models were used to calculate HR. The corresponding 95% CIs and P values of the post-RT EBV DNA model were adjusted for sex, N stage[2], pretreatment EBV DNA, and LRG-sum. The HR of the decision tree of the survival clustering analysis was adjusted for sex and N stage[2]. PFS, progression-free survival; HR, hazard ratio; CI, confidence interval; RT, radiotherapy; EBV, Epstein-Barr virus; LRG, lymph node regression grade.

=0 copies/mL but an LRG-sum >9 were assigned to the moderate-risk group according to the survival clustering analysis, which identified more patients who could potentially receive a more refined therapy on time. While most previous studies classified these patients into a low-risk group that may not need adjuvant chemotherapy, applying this methodology to stratify patients into different disease progression risk levels may assist in identifying patients at the highest risk who would benefit from subsequent adjuvant therapy and those at the lowest risk who would require a more refined follow-up strategy. Our results suggest that the combination of these three molecular and radiologic markers was more effective for outcome prediction than was post-RT EBV DNA alone and allows for a better selection of tailored surveillance schedules or more intensive adjuvant treatment. For the low-risk group (cluster 1), regular follow-ups might be considered, given the superior survival rates observed in this favorable subgroup. The medium-low risk group (cluster 2) appears to represent a subgroup with a heightened risk of occult tumor residues, which could potentially lead to tumor recurrence or metastasis. Therefore, intensified follow-ups might be an optimal strategy to explore further. Clusters 3 and 4 seem likely to experience chemotherapy resistance and/or accelerated tumor repopulation. It might be beneficial for these groups to consider alternative systemic treatments, such as immunotherapy, in combination with RT. For the most unfavorable group, cluster 4, there may particularly be a need to explore the intensification of adjuvant chemotherapy to potentially improve outcomes.

This study has some limitations that should be acknowledged. First, we employed a single-center, retrospective design; therefore, there was a possibility of bias, and the results must be validated in multicenter studies. Second, LRG was only assessed by analyzing the LN status following RT without consideration of the LN characteristics before treatment. Third, LRG score strategy simply assigns a score from 0 to 3 via the analysis of the LN regression degree according to the MRI-LRG system, which must be refined using a more sophisticated statistical analysis. Furthermore, the current evaluation of LNs is conducted in two dimensions rather than three, which could result in potentially imprecise assessments. In our future studies, we plan to use more advanced machine learning-based technologies to automatically determine the absolute volume of LNs. This advancement is expected to significantly improve the accuracy of our treatment response evaluations. Additionally, given the potential of radiomics to provide significant biological information (34) and considering the enhanced diagnostic precision offered by apparent diffusion coefficient values from diffusion-weighted imaging, incorporating three-dimensional radiomics and apparent diffusion coefficient values into our analysis represents a promising direction for subsequent research. In the future, well-designed prospective clinical studies should be undertaken to validate the efficacy of the

MRI-LRG system and survival clustering analysis-based decision tree model in discriminating patients with NPC following RT for adequate treatment guidance.

Conclusions

MRI-LRG is an effective prognosticator for patients with NPC following RT. The survival clustering analysis-based decision tree model, which jointly adopted independent prognostic factors, including LRG-sum, pretreatment plasma EBV DNA, and post-RT plasma EBV DNA, may contribute to better risk stratification and accurate treatment guidance for patients with NPC after RT.

Acknowledgments

Funding: This work was supported by the National Natural Science Foundation of China (grant number: 82171906) and the National Natural Science Foundation of China-Youth Science Fund Project (grant number: 81902638).

Footnote

Reporting Checklist: The authors have completed the STROBE reporting checklist. Available at https://qims.amegroups.com/article/view/10.21037/qims-24-275/rc

Conflicts of Interest: All authors have completed the ICMJE uniform disclosure form (available at https://qims.amegroups.com/article/view/10.21037/qims-24-275/coif). The authors have no conflicts of interest to declare.

Ethical Statement: The authors are accountable for all aspects of the work in ensuring that questions related to the accuracy or integrity of any part of the work are appropriately investigated and resolved. This study was conducted in accordance with the Declaration of Helsinki (as revised in 2013) and was approved by the Medical Ethics Committee of Sun Yat-Sen University Cancer Center (approval number: B2019-222-01). The requirement for individual consent was waived due to the retrospective nature of the study.

References

1. Wee J, Tan EH, Tai BC, Wong HB, Leong SS, Tan T, Chua ET, Yang E, Lee KM, Fong KW, Tan HS, Lee KS, Loong S, Sethi V, Chua EJ, Machin D. Randomized trial of radiotherapy versus concurrent chemoradiotherapy followed by adjuvant chemotherapy in patients with American Joint Committee on Cancer/International Union against cancer stage III and IV nasopharyngeal cancer of the endemic variety. J Clin Oncol 2005;23:6730-8.
2. Kam MK, Teo PM, Chau RM, Cheung KY, Choi PH, Kwan WH, Leung SF, Zee B, Chan AT. Treatment of nasopharyngeal carcinoma with intensity-modulated radiotherapy: the Hong Kong experience. Int J Radiat Oncol Biol Phys 2004;60:1440-50.
3. Lee AW, Sze WM, Au JS, Leung SF, Leung TW, Chua DT, Zee BC, Law SC, Teo PM, Tung SY, Kwong DL, Lau WH. Treatment results for nasopharyngeal carcinoma in the modern era: the Hong Kong experience. Int J Radiat Oncol Biol Phys 2005;61:1107-16.
4. Kwong DL, Sham JS, Au GK, Chua DT, Kwong PW, Cheng AC, Wu PM, Law MW, Kwok CC, Yau CC, Wan KY, Chan RT, Choy DD. Concurrent and adjuvant chemotherapy for nasopharyngeal carcinoma: a factorial study. J Clin Oncol 2004;22:2643-53.
5. Chi KH, Chang YC, Guo WY, Leung MJ, Shiau CY, Chen SY, Wang LW, Lai YL, Hsu MM, Lian SL, Chang CH, Liu TW, Chin YH, Yen SH, Perng CH, Chen KY. A phase III study of adjuvant chemotherapy in advanced nasopharyngeal carcinoma patients. Int J Radiat Oncol Biol Phys 2002;52:1238-44.
6. Chen L, Hu CS, Chen XZ, Hu GQ, Cheng ZB, Sun Y, et al. Adjuvant chemotherapy in patients with locoregionally advanced nasopharyngeal carcinoma: Long-term results of a phase 3 multicentre randomised controlled trial. Eur J Cancer 2017;75:150-8.
7. Hua HL, Li S, Huang H, Zheng YF, Li F, Li SL, Deng YQ, Tao ZZ. Deep learning for the prediction of residual tumor after radiotherapy and treatment decision-making in patients with nasopharyngeal carcinoma based on magnetic resonance imaging. Quant Imaging Med Surg 2023;13:3569-86.

8. Kong F, Cai B, Lin S, Zhang J, Wang Y, Fu Q. Assessment of radiotherapy combined with adjuvant chemotherapy in the treatment of patients with advanced nasopharyngeal carcinoma: a prospective study. J BUON 2015;20:206-11.
9. Yan D, Yin X, Wang L, Huang L, Tang Q, Cheng K, Yan S. Induction chemotherapy reduces target volume drift in patients with locoregionally advanced nasopharyngeal carcinoma undergoing adaptive intensity-modulated radiotherapy: a retrospective cohort study. Quant Imaging Med Surg 2023;13:1779-91.
10. Chan AT, Lo YM, Zee B, Chan LY, Ma BB, Leung SF, Mo F, Lai M, Ho S, Huang DP, Johnson PJ. Plasma Epstein-Barr virus DNA and residual disease after radiotherapy for undifferentiated nasopharyngeal carcinoma. J Natl Cancer Inst 2002;94:1614-9.
11. Li WF, Zhang Y, Huang XB, Du XJ, Tang LL, Chen L, Peng H, Guo R, Sun Y, Ma J. Prognostic value of plasma Epstein-Barr virus DNA level during posttreatment follow-up in the patients with nasopharyngeal carcinoma having undergone intensity-modulated radiotherapy. Chin J Cancer 2017;36:87.
12. Lv J, Chen Y, Zhou G, Qi Z, Tan KRL, Wang H, Lin L, Chen F, Zhang L, Huang X, Liu R, Xu S, Chen Y, Ma J, Chua MLK, Sun Y. Liquid biopsy tracking during sequential chemo-radiotherapy identifies distinct prognostic phenotypes in nasopharyngeal carcinoma. Nat Commun 2019;10:3941.
13. Chan ATC, Hui EP, Ngan RKC, Tung SY, Cheng ACK, Ng WT, Lee VHF, Ma BBY, Cheng HC, Wong FCS, Loong HHF, Tong M, Poon DMC, Ahuja AT, King AD, Wang K, Mo F, Zee BCY, Chan KCA, Lo YMD. Analysis of Plasma Epstein-Barr Virus DNA in Nasopharyngeal Cancer After Chemoradiation to Identify High-Risk Patients for Adjuvant Chemotherapy: A Randomized Controlled Trial. J Clin Oncol 2018. [Epub ahead of print]. doi: 10.1200/JCO.2018.77.7847.
14. Li WF, Zhang Y, Liu X, Tang LL, Tian L, Guo R, Liu LZ, Sun Y, Ma J. Delayed clinical complete response to intensity-modulated radiotherapy in nasopharyngeal carcinoma. Oral Oncol 2017;75:120-6.
15. Wheeler JM, Warren BF, Mortensen NJ, Ekanyaka N, Kulacoglu H, Jones AC, George BD, Kettlewell MG. Quantification of histologic regression of rectal cancer after irradiation: a proposal for a modified staging system. Dis Colon Rectum 2002;45:1051-6.
16. Salerno G, Chandler I, Wotherspoon A, Thomas K, Moran B, Brown G. Sites of surgical wasting in the abdominoperineal specimen. Br J Surg 2008;95:1147-54.
17. Patel UB, Taylor F, Blomqvist L, George C, Evans H, Tekkis P, Quirke P, Sebag-Montefiore D, Moran B, Heald R, Guthrie A, Bees N, Swift I, Pennert K, Brown G. Magnetic resonance imaging-detected tumor response for locally advanced rectal cancer predicts survival outcomes: MERCURY experience. J Clin Oncol 2011;29:3753-60.
18. Sclafani F, Brown G, Cunningham D, Wotherspoon A, Tait D, Peckitt C, Evans J, Yu S, Sena Teixeira Mendes L, Tabernero J, Glimelius B, Cervantes A, Thomas J, Begum R, Oates J, Chau I. PAN-EX: a pooled analysis of two trials of neoadjuvant chemotherapy followed by chemoradiotherapy in MRI-defined, locally advanced rectal cancer. Ann Oncol 2016;27:1557-65.
19. Patel UB, Brown G, Rutten H, West N, Sebag-Montefiore D, Glynne-Jones R, Rullier E, Peeters M, Van Cutsem E, Ricci S, Van de Velde C, Kjell P, Quirke P. Comparison of magnetic resonance imaging and histopathological response to chemoradiotherapy in locally advanced rectal cancer. Ann Surg Oncol 2012;19:2842-52.
20. Liu SL, Sun XS, Li XY, Tang LQ, Chen QY, Lin HX, Liang YJ, Yan JJ, Lin C, Guo SS, Liu LT, Li Y, Xie HJ, Tang QN, Liang H, Guo L, Mai HQ. The diagnostic and prognostic values of plasma Epstein-Barr virus DNA for residual cervical lymphadenopathy in nasopharyngeal carcinoma patients: a retrospective study. Cancer Commun (Lond) 2019;39:14.
21. Li WZ, Liu GY, Lin LF, Lv SH, Qiang MY, Lv X, Wu YS, Liang H, Ke LR, Wang DL, Yu YH, Qiu WZ, Liu KY, Guo X, Li JP, Zou YJ, Xiang YQ, Xia WX. MRI-detected residual retropharyngeal lymph node after intensity-modulated radiotherapy in nasopharyngeal carcinoma: Prognostic value and a nomogram for the pretherapy prediction of it. Radiother Oncol 2020;145:101-8.
22. Zhu Y, Luo C, Zhou S, Li H, Liu L, Kou KI, Lei F, Zhang G, Cao D, Liang Z. Optimal Size Threshold for MRI-Detected Retropharyngeal Lymph Nodes to Predict Outcomes in Nasopharyngeal Carcinoma: A Two-Center Study. AJR Am J Roentgenol 2024;222:e2329984.
23. Li HJ, Hu YY, Huang L, Zhou J, Li JJ, Xie CB, Chen MY, Sun Y, Liu LZ, Tian L. Subclassification of skull-base invasion for nasopharyngeal carcinoma using cluster, network and survival analyses: A double-center retrospective investigation. Radiother Oncol 2019;134:37-43.
24. Tang LL, Chen YP, Mao YP, Wang ZX, Guo R, Chen L, Tian L, Lin AH, Li L, Sun Y, Ma J. Validation of the 8th Edition of the UICC/AJCC Staging System for Nasopharyngeal Carcinoma From Endemic Areas in the Intensity-Modulated Radiotherapy Era. J Natl Compr

Canc Netw 2017;15:913-9.
25. Lambregts DMJ, Boellaard TN, Beets-Tan RGH. Response evaluation after neoadjuvant treatment for rectal cancer using modern MR imaging: a pictorial review. Insights Imaging 2019;10:15.
26. Rödel C, Martus P, Papadoupolos T, Füzesi L, Klimpfinger M, Fietkau R, Liersch T, Hohenberger W, Raab R, Sauer R, Wittekind C. Prognostic significance of tumor regression after preoperative chemoradiotherapy for rectal cancer. J Clin Oncol 2005;23:8688-96.
27. Kalisz KR, Enzerra MD, Paspulati RM. MRI Evaluation of the Response of Rectal Cancer to Neoadjuvant Chemoradiation Therapy. Radiographics 2019;39:538-56.
28. Lee HG, Kim SJ, Park IJ, Hong SM, Lim SB, Lee JB, Yu CS, Kim JC. Effect of Responsiveness of Lymph Nodes to Preoperative Chemoradiotherapy in Patients With Rectal Cancer on Prognosis After Radical Resection. Clin Colorectal Cancer 2019;18:e191-9.
29. Coskun HH, Ferlito A, Medina JE, Robbins KT, Rodrigo JP, Strojan P, Suárez C, Takes RP, Woolgar JA, Shaha AR, de Bree R, Rinaldo A, Silver CE. Retropharyngeal lymph node metastases in head and neck malignancies. Head Neck 2011;33:1520-9.
30. Jiang F, Jin T, Feng XL, Jin QF, Chen XZ. Repeat biopsy of primary disease negatively affects the outcome of patients with nasopharyngeal cancer treated with definitive intensity-modified radiotherapy: a cohort analysis of 795 patients. Jpn J Clin Oncol 2016;46:435-40.
31. Pramanik R, Arora S, Sharma P, Biswas A, Nayak B, Thakar A, Sharma A, Ghose S. Cell-free EBV DNA as a biomarker during clinical management of nasopharyngeal carcinoma in a nonendemic region. J Med Virol 2022;94:720-8.
32. Lee VH, Kwong DL, Leung TW, Choi CW, O'Sullivan B, Lam KO, Lai V, Khong PL, Chan SK, Ng CY, Tong CC, Ho PP, Chan WL, Wong LS, Leung DK, Chan SY, So TH, Luk MY, Lee AW. The addition of pretreatment plasma Epstein-Barr virus DNA into the eighth edition of nasopharyngeal cancer TNM stage classification. Int J Cancer 2019;144:1713-22.
33. Hui EP, Li WF, Ma BB, Lam WKJ, Chan KCA, Mo F, Ai QYH, King AD, Wong CH, Guo R, Poon DMC, Tong M, Li L, Lau TKH, Wong KCW, Lam DCM, Lo YMD, Ma J, Chan ATC. Integrating postradiotherapy plasma Epstein-Barr virus DNA and TNM stage for risk stratification of nasopharyngeal carcinoma to adjuvant therapy. Ann Oncol 2020;31:769-79.
34. Wang T, Li YY, Ma NN, Wang PA, Zhang B. A MRI radiomics-based model for prediction of pelvic lymph node metastasis in cervical cancer. World J Surg Oncol 2024;22:55.

Cite this article as: Yang H, Liang Z, Liang J, Cao D, Cao Q, Zhao F, Zhang W, Kou KI, Cui C, Liu L, Li H, Peng Z, Zhu S. A magnetic resonance imaging-based lymph node regression grading scheme for nasopharyngeal carcinoma after radiotherapy. Quant Imaging Med Surg 2024;14(8):5513-5525. doi: 10.21037/qims-24-275

